Lock-In Pixel CMOS Image Sensor for Time-Resolved Fluorescence Readout of Lateral-Flow Assays

Alexander Hofmann, Benjamin Saft, Peggy Reich, Martin Grabmann, Georg Gläser, Max Trübenbach, Alexander Rolapp, Marco Reinhard, Friedrich Scholz, and Eric Schäfer

***Abstract*—We present a CMOS image sensor (CIS) based time-resolved fluorescence (TRF) measurement system for filter-less, highly sensitive readout of lateral-flow assay (LFA) test strips. The CIS contains a 256 × 128 lock-in pixel (LIP) sensor array. Each pixel has a size of 10 μm × 10 μm and includes a photodiode acting as signal transducer. The LIP CIS was designed in a standard 0.18 μm CMOS technology specifically for TRF applications. The LIP architecture blocks interfering light when fluorophores are excited and accumulates the emitted fluorescence light to be measured over multiple cycles after excitation. This allows to detect even small amounts of fluorescence light over a wide analyte concentration range. The LIP CIS based TRF reader was characterized in terms of reproducible and uniform signal intensities with use of appropriate Europium(III) [Eu 3+] chelate particles as fluorescence standards. We measured different concentrations of Eu-based nanoparticles (NP) on test strips with the TRF reader. The sensor system shows 5.1 orders of magnitude of detection dynamic range (DDR) with a limit of detection (LoD) of 0.1 ng/cm. In addition, using human C-reactive protein (hCRP) as a model analyte, we compared the developed TRF reader with a commercial colorimetric LFA reader. For the quantification of CRP, the LIP CIS based TRF reader demonstrates a DDR of 3.6 orders of magnitude with an excellent LoD of 0.05 ng/mL, which is 14 times better than the LoD of the commercial LFA reader.**

***Index Terms*—Lock-in pixel, CMOS image sensor, TRF, no filter, Eu nanoparticle, photodiode, point-of-care, immunoassay, LFA.**

Manuscript received 2 March 2022; revised 30 May 2022; accepted 27 June 2022. Date of publication 21 July 2022; date of current version 10 October 2022. This work was supported by the German Land of Thüringen and in part by the European Union Funds through the European Regional Development Fund (ERDF) under Grant 2017 FE 9044. This paper was recommended by Associate Editor Chung-Chih Hung. *(Corresponding author: Alexander Hofmann.)*

Alexander Hofmann, Benjamin Saft, Martin Grabmann, Georg Gläser, Alexander Rolapp, Marco Reinhard, and Eric Schäfer are with the IMMS Institut für Mikroelektronik- und Mechatronik-Systeme gemeinnützige GmbH (IMMS GmbH), 98693 Ilmenau, Germany (e-mail: alexander.hofmann@imms.de; benjamin.saft@imms.de; martin.grabmann@imms.de; georg.glaeser@imms.de; alexander.rolapp@imms.de; marco.reinhard@imms.de; eric.schaefer@imms.de).

Peggy Reich was with the IMMS Institut für Mikroelektronik- und Mechatronik-Systeme gemeinnützige GmbH (IMMS GmbH), 98693 Ilmenau, Germany (e-mail: reichpeggy@gmail.com).

Max Trübenbach is with the Senova Gesellschaft für Biowissenschaft und Technik mbH, 99427 Weimar, Germany (e-mail: m.truebenbach@senova.de).

Friedrich Scholz was with the Senova Gesellschaft für Biowissenschaft und Technik mbH, 99427 Weimar, Germany. He is now with Abbott Rapid Diagnostics Jena GmbH, 07743 Jena, Germany (e-mail: friedrich-scholz@gmx.de).

Color versions of one or more figures in this article are available at https://doi.org/10.1109/TBCAS.2022.3192926.

Digital Object Identifier 10.1109/TBCAS.2022.3192926

I. Introduction

DURING the Corona pandemic, lateral-flow assay (LFA) strip tests became the gold standard for self and rapid testing. These low-cost tests are easy to use and indicate the presence of an infection with SARS-CoV-2. LFA test strips alone, however, cannot detect low viral loads, and they currently only offer a yes/no or at least a semi-quantitative answer about the presence of the virus [1].

LFA test readers, instead, provide the option of quantitative detection of pathogens based on optical readout of the strips, and they can be deployed right at the point-of-care (PoC). Most LFA test readers brought to market in recent years are based on colorimetric measurement of LFAs with gold nanoparticles (NP) [2]. For COVID-19 rapid tests, gold NP are also the labeling standard. Although fluorescence-based LFA readers promise higher sensitivities [2]–[4], only a few systems are commercially available. Perhaps one main reason is that these test devices often require expensive optical filters to reduce the influence of excitation light and background fluorescence. Due to their large Stokes shifts (≈ 300 nm) and long decay times (10 . . . 1000 μs) [3], lanthanide markers such as Europium (Eu) allow for more moderate readout requirements. Weight, size, and cost of fluorescence readers can be greatly reduced by combining time-resolved optical measurement using optoelectronic CMOS sensors and Eu-based markers. CMOS-based sensor systems can be miniaturized and fabricated at low cost and thus be employed to transfer measurement technology to the PoC, which is otherwise only accessible to central laboratories.

Using time-resolved fluorescence (TRF) measurement techniques, latest developments showcase the highly sensitive detection of biochemical signals, capturing the nanosecond decay of fluorescent dyes within picoseconds [5]–[7]. Until now, high system costs and complexity due to lenses, mirrors, and filters, among others, as well as high-power excitation laser sources have prevented TRF from being used cost-effectively in PoC applications. Optical detectors like charge-coupled devices (CCD), photomultiplier tubes (PMT) or single-photon avalanche diodes (SPAD) are often used in TRF, but they have high bias voltages and expensive fabrication processes. On the other hand, TRF shows the potential to reduce overall system costs by eliminating the need for a variety of optics, including optical filters.

TRF systems with SPADs that do not use optical filters [7]–[9] are very well suited for the detection of low fluorescence intensities. On the other hand, these systems have a restricted optical dynamic range [9], [10]. This limits their use for detecting high concentrations of fluorescent particles in bio-analytical applications with high dynamic ranges. For proteomic assays, for example, the detection range can be over several orders of magnitude [11]. Additionally, SPAD detectors often need special cooling techniques to reduce noise in terms of dark count rate to guarantee highly sensitive single-photon detection [12] as well as expensive manufacturing processes that increase the overall costs of the system. For the detection of low fluorophore concentrations, state-of-the-art low-cost TRF readers still require optical filters and have a limited detection range [13].

In this work, we present the design, implementation, and evaluation of a filter-less, miniaturized lock-in pixel (LIP) CMOS image sensor (CIS) based TRF reader for highly sensitive readout of analytes on LFA test strips over a wide concentration range. In our work in [14], we showed the great potential of a CMOS sensor ASIC-based TRF reader system to improve the biochemical analysis process in PoC applications. In comparison, in this work we describe a completely new LIP CIS based TRF reader. The sensor system was designed in a cost effective standard CMOS technology specifically for TRF measurements. Our work was inspired by the excellent performance of LIP CIS in terms of dynamic range and SNR in fluorescence applications, known from the work of [6] and [15].

In filter-less TRF applications it is crucial to eliminate interfering background illumination of the light source during the measurement. Therefore the LIP architecture allows to firstly block incoming interfering light while the fluorophores are excited and secondly accumulate the emitted fluorescence light to be measured over multiple cycles after excitation. This leads to detection of even small amounts of fluorescence light over a wide concentration range of analytes. In addition, with the large 256×128 LIP sensor array the whole test line of the LFA test strips can be imaged. This helps to capture fluorescence light over a larger test line area.

Since TRF measurements are time-critical, the digital logic inside the ASIC precisely synchronizes the light source with the time-resolved detection on the LIP CIS. To reduce overall system costs we use a low-cost LED light source instead of an expensive pulsed laser.

We developed an assay for the detection of human C-reactive protein (CRP) to prove the performance of our TRF image sensor system. A rising CRP level in the blood indicates inflammation, infection, and non-infectious disease. Fig. 1 shows the time-resolved measurement principle for the quantification of CRP with the LIP CIS. First, a sample with CRP is added to the sample pad of the test strip. The sample is dragged through the conjugate pad by the capillary forces of the LFA nitrocellulose strip, and the CRP binds to the Eu-labeled anti-CRP Ab. On the test line with anti-CRP Ab, only as many Eu conjugates can bind to CRP as are contained in the sample. No Eu conjugates with or without CRP can bind in the reference area because the membrane is not coated and no capture Ab are immobilized there. Therefore, the reference area acts as a dark signal reference. An ultraviolet (UV) LED with a wavelength of $365\ \mathrm{nm}$ excites the captured Eu particles.

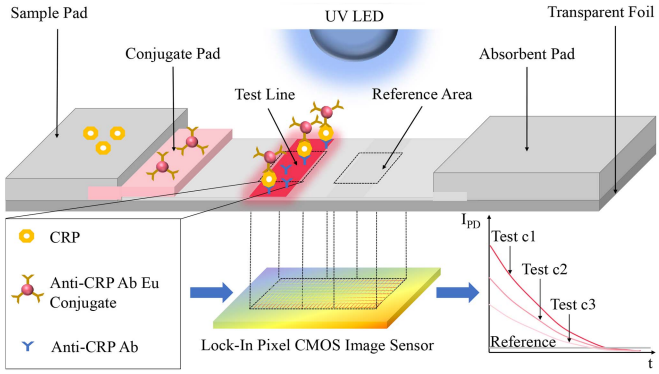

Fig. 1. Time-resolved measurement principle for quantification of CRP with Eu conjugates by measuring fluorescence on LFA test strips using the LIP CIS and an UV-LED. Optical components (lenses etc.) are not shown here. Modified from [14].

The test lines emit light of varying intensity depending on the bound CRP concentration at a wavelength of $613\ \mathrm{nm}$ once the LED is turned off. The fluorescence intensity of the test lines differs according to the bound concentration of CRP with Eu particles. The dark reference of the reference area and the fluorescence of the test line are imaged. For quantification of Eu NP and CRP, LFA test strips were provided by Senova Gesellschaft für Biowissenschaft und Technik mbH, Weimar, Germany.

This paper is organized as follows: The new LIP CIS based TRF reader is presented in Section II and new performance data of the LIP CIS TRF reader in comparison to the results of our work in [14] and to a commercial LFA reader are shown in Section IV. Design and function of the new ASIC and of all system components are described in Section II-A and in Section II-B, respectively. The developed lateral flow assay for the detection of CRP by TRF measurement, including the chemicals used, Ab conjugation with Eu particles and preparation of the test strips, is described in Section III-A and Section III-B. Section IV-A proves the functionality of the system and shows the results for the detection of different concentrations of Eu particles. Section IV-B presents the quantification of different CRP concentrations on LFA test strips using the filter-less LIP CIS TRF reader compared to the CMOS sensor ASIC-based TRF reader in [14] as well as to a commercially available colorimetric LFA reader. The results of this work are discussed and compared to the state of the art in Section V and final conclusions are drawn in Section VI.

II. System Description

A. Lock-In Pixel CMOS Image Sensor ASIC

The LIP CIS was developed with a variety of diagnostic applications in mind, such as readout of LFAs as discussed in this work.

The imager has a resolution of 256×128 pixels with a pixel size of $10\ \mu\mathrm{m} \times 10\ \mu\mathrm{m}$. The chip size is $3.65\ \mathrm{mm} \times$

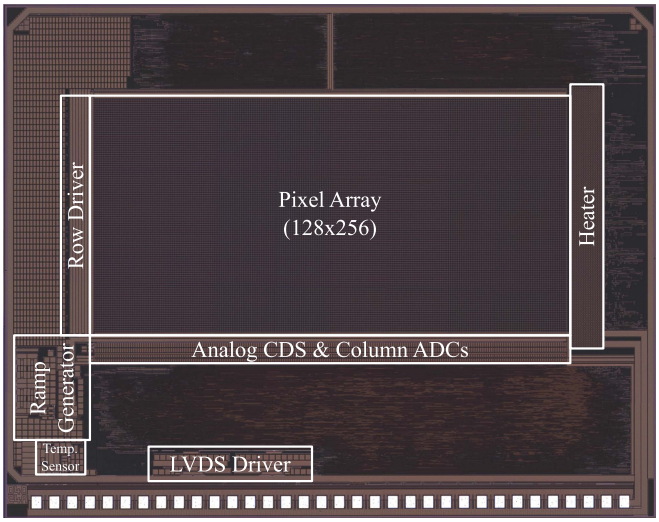

Fig. 2. Micrograph of the LIP CIS with major blocks needed for the complete image acquisition process. The resistance heater has been integrated for microfluidic applications (not used for this work) to heat the surrounding fluids if needed.

TABLE I
CHARACTERISTICS OF THE DEVELOPED LIP CIS

Technology	0.18 µm CMOS
Supply voltage	3.3 V
Die area	3.65 mm × 2.8 mm
Array dimensions	256 × 128 pixels
Photodiode	10 µm × 10 µm
Photodiode quantum efficiency	73 % @ $\lambda = 600$ nm
Photodiode dark current	200 e^-/s
Charge conversion gain	27 µV/e^-
Full-well capacity	53 ke^-
Pixel fill factor	59 %
Frame rate	24 Hz

2.8 mm. It was manufactured in a commercial 180 nm CMOS technology. A micrograph is shown in Fig. 2. Table I summarized the characteristics of the ASIC.

The CIS integrates a LIP array together with an analog correlated double sampling (CDS) stage, 256 analog-to-digital converters (ADCs), and a flexible digital control logic. The analog pixel signals are converted column-wise by 12-bit single-slope ADCs with a LSB of 90 µV. These converters share a common voltage ramp signal which is compared to the sampled pixel voltages. A block diagram of the signal chain is shown in Fig. 3. A global comparator starts all column counter simultaneously once the reference voltage V_{Ref} is crossed. As soon as the ramp voltage reaches the sampled value of the particular column, it's comparator stops the column counter and latches the final value which is processed afterwards. For observing and calibrating, if needed, an analog temperature sensor is included. The image acquisition process is orchestrated by a programmable on-chip digital pattern generator which allows a highly flexible adjustment of digital waveforms and timings. This unit also controls the included UART for transmitting the data to the measurement system. To enable a higher frame rate, the UART can be driven at a data rate up to 50 MBps. The overall configuration is set

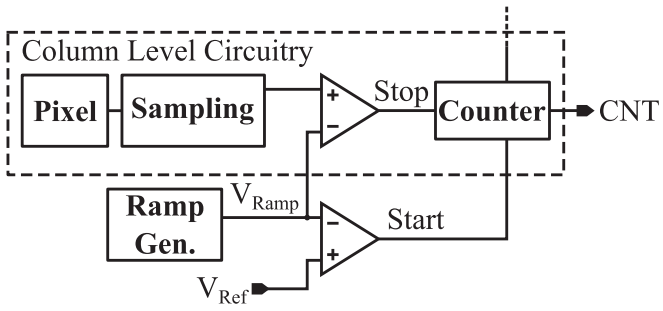

Fig. 3. Block diagram of the signal chain. The column level circuit comprises the pixel, the CDS sampling stage, a comparator, and a counter. On top level, a ramp generator and a comparator control the start of the column count.

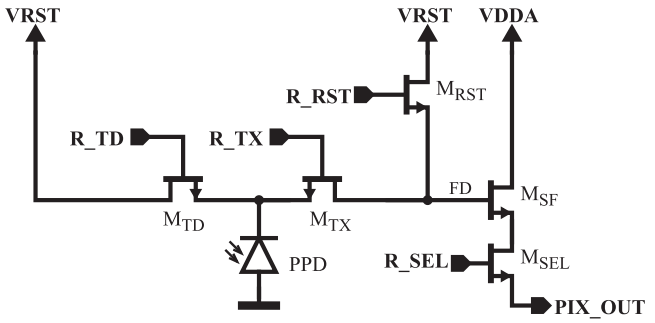

Fig. 4. Schematic of the LIP. During excitation of the fluorescent dye, M_{TD} leads the generated charge carriers to VRST while M_{TX} is high ohmic. Once the excitation light is off, M_{TD} is high ohmic and M_{TX} leads the charge carriers to the accumulation node FD. M_{SF} and M_{SEL} are used to read the pixel and M_{RST} resets it.

up via an I2C interface for programming the pattern generator and accessing internal register values. Hence, the chip can be employed in most measurement systems as long as they provide an I2C master and an UART interface on the digital side.

The core of the ASIC is the LIP architecture. The pixel is built around a pinned photodiode (PPD) acting as light-sensitive element, see Fig. 4 and Fig. 5. Two rapidly switchable taps (M_{TX}, M_{TD}) are connected to this diode in order to separate the charge carriers generated by the incident light into two temporal components. While the fluorescent Europium-based dyes are excited by a light pulse, the incident excitation light is substantially suppressed by sinking the charge carriers to VRST (M_{TD} conductive). Once the light source is switched off and the excitation light has decayed (see t_{wait} in Fig. 6 (a)), the tap configuration in the pixel is swapped (M_{TX} conductive). Following, the emission light is collected (accumulation takes place on the capacitance of node FD) until the emission light also has decayed (t_{integ}).

This sequence can be repeated several times, as shown in Fig. 6 (b), to accumulate the charges generated by the fluorescent light on the pixel's FD node. Especially in very-low light scenarios, this multiple-excitation mode realizes a first step of signal amplification before the signal is further processed or digitized and leads to increased signal-to-noise ratios. Subsequently, the accumulated charges in the pixel array are converted row by row (using M_{RST}, M_{SF}, and M_{SEL}), and the image data is transmitted

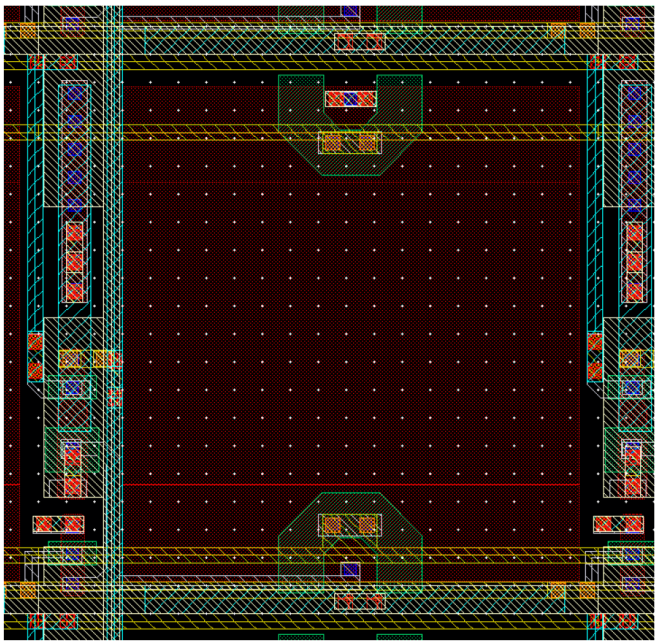

Fig. 5. Layout of the LIP. On the top and bottom edge are the transistors M_{TD} and M_{TX}, respectively. The rest of the pixel circuit is located at the left edge. The pixel has a fill factor of $59\,\%$.

at the end of the capturing cycle. The level of the reset voltage VRST and the pixel supply voltage VDDA are both $3.3\,\mathrm{V}$. The signal level for R_{TD}, R_{TX}, and R_{SEL} are $0\,\mathrm{V}$ or $3.6\,\mathrm{V}$.

B. Time-Resolved Measurement System

We used a Xilinx ZYNQ SoC platform to implement a measurement system for evaluation and demonstration of the LIP CIS with real LFAs and to compare it with other readers. The system's block diagram is shown in Fig. 7. The SoC-integrated FPGA was used for pre-silicon prototyping and allowed better debugging of the initial setup. For operation with the CIS, the FPGA is not necessary. A Linux-based OS is run on the embedded ARM core of the ZYNQ and hosts a Python program for the application-oriented evaluation of the image sensor. The demonstrator system provides a WiFi interface for wireless configuration of the sensor and image readout, through which the user can interact with the chip via a web browser.

The hardware is housed in a 3D-printed light-proof case together with a pulsed LED light source for excitation of the fluorescent dyes, see Fig. 8.

One major challenge during the design of the demonstrator was the pulsed UV-LED light source. It needs to have a fast switch-off time which is well below the decay times of EU-based fluorescent dyes. Therefore, we employ a H-bridge circuit to reverse the LED polarity during switching and thus actively flushing the charge carriers out of the LED. This enables switch-off times of approximately $10\,\mathrm{ns}$ at a wavelength of $365\,\mathrm{nm}$ and a light power of approximately $3\,\mathrm{W}$. In order to compensate for aging and variations in LED brightness, conventional blank images are captured which can be used to calibrate the fluorescence images.

The LIP CIS IC itself is glued on and wire-bonded to an application-specific cartridge PCB that can be plugged into the demonstrator. Two types of cartridges were designed. The first type is intended for LFA test strip measurements and makes use of a M12 lens that is mounted above the CIS. Fig. 9 shows the setup with a LFA test strip with an Eu line, being excited with UV light and emitting red light, mounted in the focal plane of the lens cartridge.

To get an impression of the TRF images that the CIS can capture within the demonstration platform, Fig. 10 shows sample images of LFA test strips with Eu lines of different concentrations. For very low Eu concentrations, like in Fig. 10 (b), the non-ideal suppression of the the emission light, i.e. the background signal, leads to a blurry line with low contrast. This parasitic effect is caused by charges leaking through to the FD node within the pixel during the excitation phase of the illumination cycle.

III. Lateral-Flow Assay Protocol

A. Antibody Conjugation to Europium Nanoparticles

The covalent coupling of anti-human CRP Ab to carboxyl-functionalized Europium nanoparticles (Fig. 11 (a)) was realized by using the 1-Ethyl-3-(3-dimethylaminopropyl) carbodiimid (EDC)/Sulfo-N-Hydroxysulfosuccinimid (s-NHS) method as described in [23]. For the activation of the caboxyl group $1\,\mathrm{mg}$ Europium chelate nanoparticle (diameter $100\,\mathrm{nm}$, carboxyl-functionalized) was mixed with $50\,\mu\mathrm{L}$ of $100\,\mathrm{mM}$ 2-(N-morpholino)ethanesulfonic acid (MES) buffer (pH 5.5) and $10\,\mu\mathrm{L}$ of an EDC/s-NHS solution (5 mg/mL) was added. The mixture was incubated at room temperature (RT). Then, the excess of EDC/s-NHS was removed by multiple washing steps through centrifugation and re-dispensed in $0.5\,\mathrm{mL}$ $\mathrm{ddH_2O}$. The pH value was adjusted by adding $100\,\mu\mathrm{L}$ $120\,\mathrm{mM}$ Phosphat buffered saline (PBS) (pH 7.2). $20\,\mu\mathrm{g}$ of monoclonal anti-human CRP detection Ab was added to the activated Europium beads and incubated for $1\,\mathrm{h}$. After centrifugation the supernatant was discarded and the precipitate was washed with $\mathrm{ddH_2O}$. The conjugate was finally taken up in $0.25\,\%$ (w/v) bovine serum albumin (BSA) solution in $\mathrm{ddH_2O}$.

B. Preparation of Lateral Flow Test Strips

A lateral flow test strip consists of a sample pad, conjugate release pad, nitrocellulose membrane, and absorbent pad attached onto a backing card. The capture Ab are immobilized on the nitrocellulose membrane via passive adsorption. The nitrocellulose membrane was coated with monoclonal anti-human CRP capture Ab (test line) and goat anti-mouse IgG (control line) in $10\,\mathrm{mM}$ PBS pH 7.2 by using a Biodot XYZ-3000 dispensing platform. Afterwards the membrane was dried at $37\,^{\circ}\mathrm{C}$ for $2\,\mathrm{h}$. The antibody-conjugated europium nanospheres were diluted in PBS buffer ($30\,\mathrm{mM}$, pH 7.2) with $1\,\%$ (w/v) BSA and $1\,\%$ (w/v) sucrose and sprayed onto a fiber glass membrane with a Biodot XYZ-3000 dispensing platform to a final concentration of $0.05\,\mu\mathrm{g/cm}$. The conjugate pads were dried for $2\,\mathrm{h}$ at $37\,^{\circ}\mathrm{C}$. The coated nitrocellulose membrane and the absorption pad were

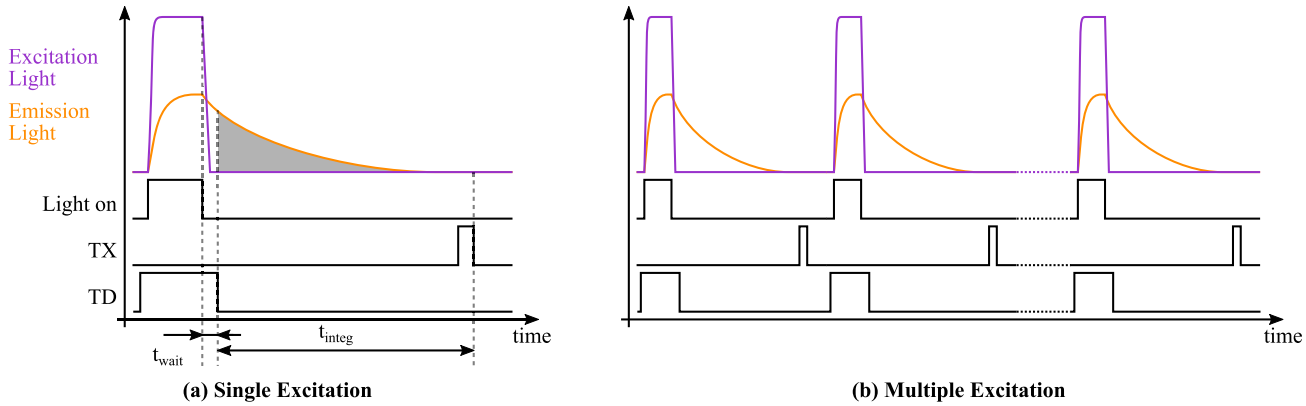

Fig. 6. Timing diagrams for the fluorescence readout process. In (a), a normal, single-excitation process is shown. The LIP features the multiple excitation process shown in (b) where the generated charge is accumulated over several cycles.

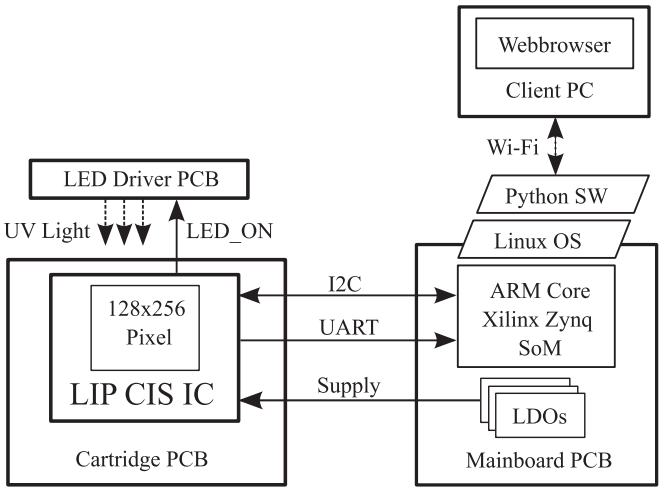

Fig. 7. Block diagram of the evaluation and demonstration platform.

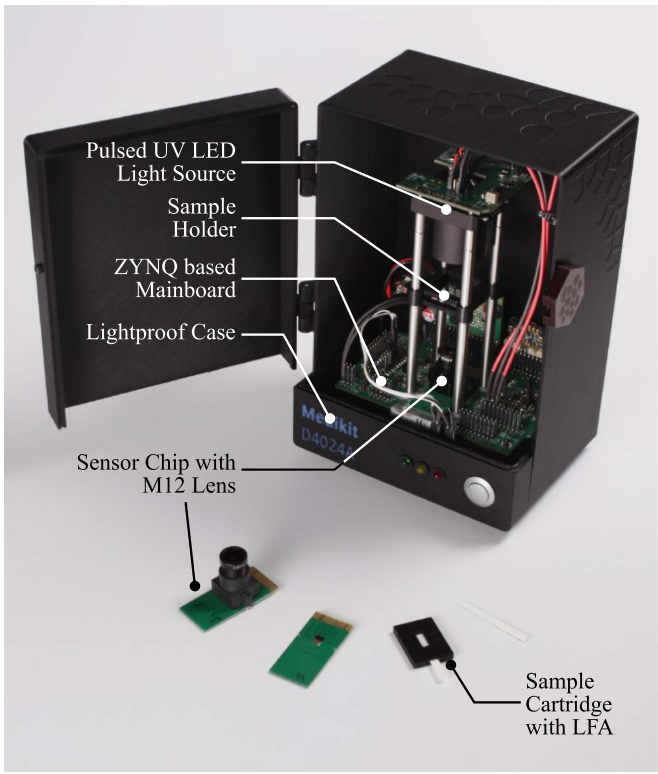

Fig. 8. Demonstrator platform of the time resolved measurement system. The box houses a ZYNQ-based system, the excitation UV-LED light source and the chip cartridge with a lens (shown in the foreground).

first attached onto the backing card. Then the loaded conjugate pads and the sample pad (untreated glass fiber membrane) were also fixed onto the backing card and cut into test strips ($4\ \mathrm{mm} \times 60\ \mathrm{mm}$) using a Biodot CM4000 guillotine Cutter. The general concept of the antibody-antigen interaction of the lateral flow test strip is shown in Fig. 11 (b).

All required reagents and membrane materials were received from Senova Gesellschaft für Biowissenschaft und Technik mbH (Weimar, Germany).

IV. Measurement Results

A. System Validation With Fluorescence Standards

To test our image sensor and to verify its functionality, we made measurements with Eu particles on test strips. First, solutions containing Eu particles were dropped onto a lateral flow test and then dried. In the measurement setup, we used a transmitted light configuration in which the lateral flow test strip was inserted between the light source and the CIS. The substrate of the strip was transparent. For this setup, lenses were used to collimate and focus the light onto the lateral flow test and to image the strip onto the CIS IC. The calibration curve and standard deviation of the measurement points of the LIP CIS TRF reader for the measurement of fluorescence standards for different excitation modes are presented in Fig. 12 (a). Fig. 12 (b) shows the normalized calibration curves of the LIP CIS based TRF reader using fluorescence standards (light grey, square) in comparison to the normalized calibration curves of the CMOS sensor ASIC TRF reader from our previous work [14] (grey, triangle) for the quantification of different Eu particle concentrations. Test strip images of the LIP CIS based TRF reader for different excitation

Fig. 9. Europium labeled LFA inserted in the demonstrator platform. The LFA is mounted in the focal plane of the lens.

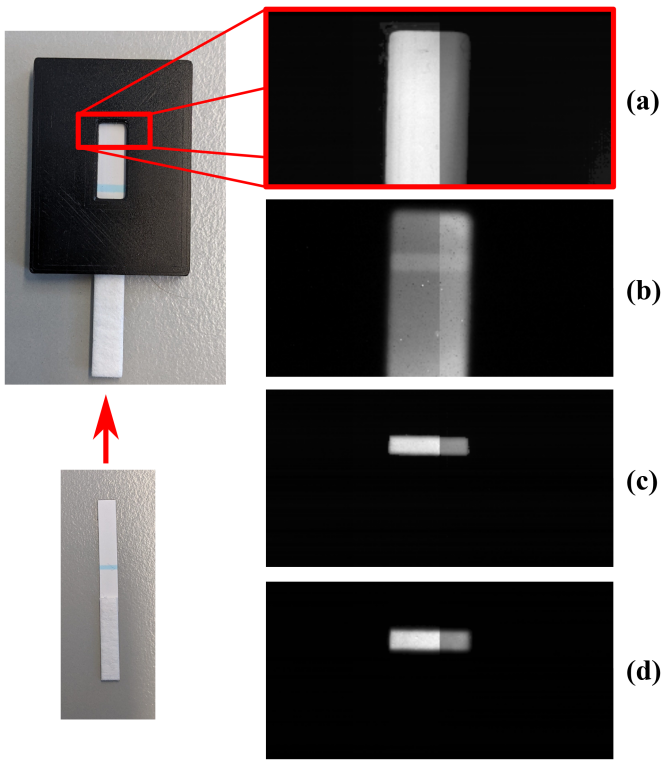

Fig. 10. Example TRF images of the sensor system taken of LFA test strips with Eu lines of different concentrations. (a) Reference image (no fluorescence/background lightening): the vertical line is caused by two different pixel variants with slightly different parameters, in the image field (b) Low concentration (1 ng/cm, 78 illumination cycles, 2.8 ms LED on time): the background of the LFA is shining through since the suppression of the excitation light is not 100 % perfect; (c) Medium concentration (50 ng/cm, 1 illumination cycle, 2.8 ms LED on time); (d) High concentration (6 µg/cm, 1 illumination cycle, 23 µs LED on time).

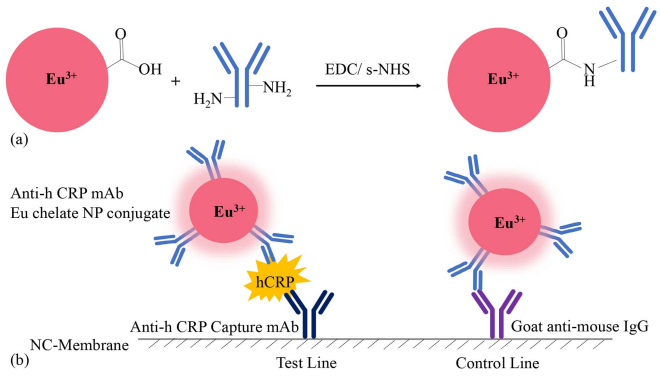

Fig. 11. (a) Reaction scheme for the covalent coupling of Ab to carboxyl-functionalized Europium chelate nanoparticles using EDC/ s-NHS chemistry. (b) Schematic illustration of the antibody-antigen interaction within a CRP specific lateral flow test strip using Europium chelate nanoparticles.

modes and Eu particle concentrations used for the quantification are shown in Fig. 12 (c).

The image sensor based TRF reader shows a very high DDR of 5.1 orders of magnitude and a LoD of 0.1 ng/cm compared to the TRF reader with CMOS sensor ASIC from [14] with a DDR of 4.4 orders of magnitude and a LoD of 0.5 ng/cm. The calibration curves were calculated with a four parameter logistic function (4-PL) as nonlinear regression which is a standard curve-fitting method for ELISA [16]. To obtain the overall run-to-run coefficient of variation (CV) across all concentrations, those measured values that had an individual CV of $\leq 30\,\%$ for each concentration were considered. For measurements of fluorescence standards with three LFA test strips per concentration (three-fold determination) the overall run-to-run CV for the CMOS sensor ASIC based TRF reader of [14] is $5.8\,\%$. In comparison, the overall run-to-run CV for the LIP CIS TRF reader of this work with 8 LFA test strips per concentration (8-fold determination) is $1.8\,\%$.

The values in Fig. 12 (a) and Fig. 12 (b) are obtained from the images shown in Fig. 12 (c) by averaging over a selected area of pixel within the relevant region of the image, see the squares on the right-hand side. The measurement result in Fig. 12 (a) is the ratio of the average value in the test line area to the average value in the reference area. The normalized signals in Fig. 12 (b), are the ratios normalized to their maximum values. With decreasing concentration of the Eu particles, the number of excitations has been increased in order to accumulate sufficient charge carriers in the LIP. Thus, even weak fluorescence signals from the test strips could be detected. However, the SNR and thus the LoD is limited by the increasing background signal of the test strip when detecting lower concentrations of Eu particles in the multiple-excitation mode.

B. Quantification of CRP

We also quantified Eu-labeled CRP lateral flow test strips with the demonstrator system. With these measurements we demonstrate the suitability of the improved LIP CIS-based TRF reader for PoC tests. For this case, the intra-assay variation of the LFA is inherently included in the measurement results.

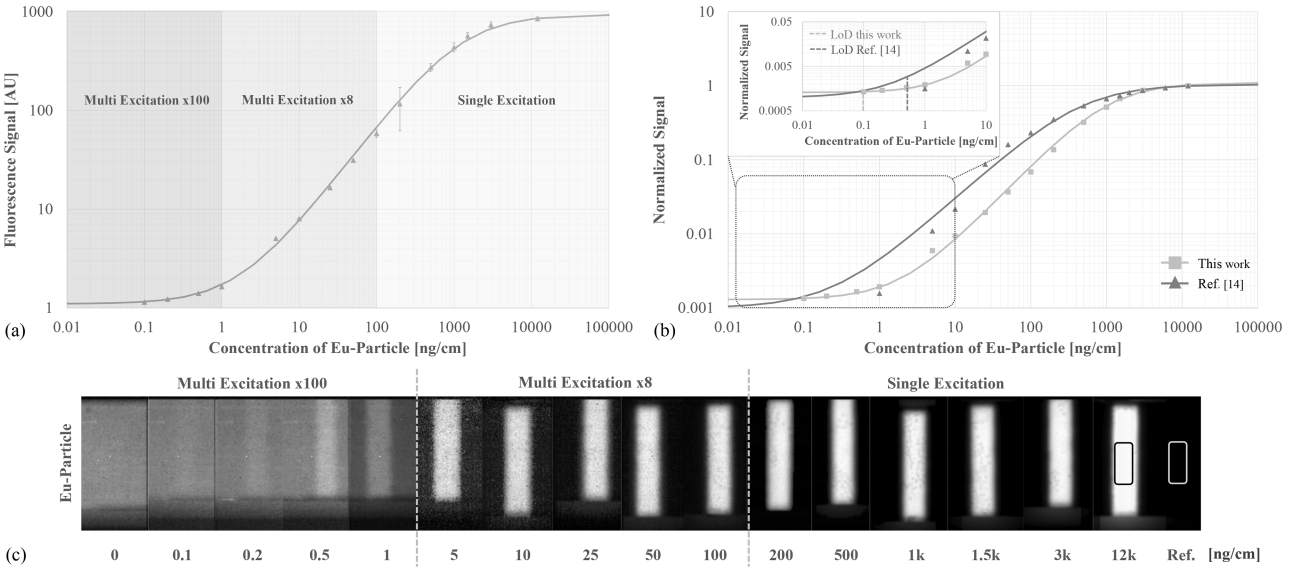

Fig. 12. (a) Calibration curve and standard deviation of the measurement points of the LIP CIS TRF reader using fluorescence standards for concentrations of 12 µg/cm, 3 µg/cm, 1.5 µg/cm, 1 µg/cm, 500 ng/cm, 200 ng/cm, 100 ng/cm, 50 ng/cm, 25 ng/cm, 10 ng/cm, 5 ng/cm, 1 ng/cm, 0.5 ng/cm, 0.2 ng/cm, 0.1 ng/cm, and of the control (0 ng/cm) for different excitation modes. (b) Normalized calibration curves of the image sensor based TRF reader with a LoD of 0.1 ng/mL with fluorescence standards (light grey, square) compared to the normalized calibration curves of the CMOS sensor ASIC TRF reader from [14] with a LoD of 0.5 ng/mL using fluorescence standards for concentrations of 12 µg/cm, 6 µg/cm, 3 µg/cm, 2 µg/cm, 1.5 µg/cm, 1 µg/cm, 500 ng/cm, 200 ng/cm, 100 ng/cm, 50 ng/cm, 25 ng/cm, 10 ng/cm, 5 ng/cm, 1 ng/cm, and of the control (0 ng/cm) (grey, triangle). (c) Images of the LIP CIS TRF reader for the measured concentrations and the reference for different excitation modes of single, x8 and x100 UV light excitation.

Therefore, these results will show higher variations compared to the tests with fluorescence standards.

The measured CRP concentrations with Eu particles are shown in Fig. 13 together with results for the CMOS sensor ASIC based TRF reader from [14] and with results for a commercially available LFA reader from Qiagen [17] using a conventional colorimetric gold NP LFA. They were calculated using a 4-PL as nonlinear regression. All LFA test strips for this comparison were provided by Senova. The LFA test strips with gold NP labeling were prepared equivalent to those with Eu particles for CRP. CRP concentrations were measured using an 11-fold determination.

As with the validation of the system with fluorescent standards, the background signal of the test strips increases as the CRP concentration decreases, limiting the SNR and LoD. In addition, inhomogeneous light distributions of fluorescence for the measured CRP concentrations can be seen in the test line region as a result of the intra-assay and test strip variations.

The LIP-CIS based TRF reader demonstrates a DDR of 3.6 orders of magnitude with a very good LoD of 0.05 ng/mL. The overall run-to-run CV is 20 %. On the other hand, the CMOS sensor system from [14] has a DDR of 3.3 orders of magnitude with a LoD of 0.2 ng/mL and an overall run-to-run CV of 26 %. The colorimetric LFA reader system achieved a DDR of around 2.5 orders of magnitude, a LoD of 0.7 ng/mL and an overall run-to-run CV of 11 %. These performance data of the reader systems were determined using buffer samples, and LoDs were calculated from the mean value plus three times the standard

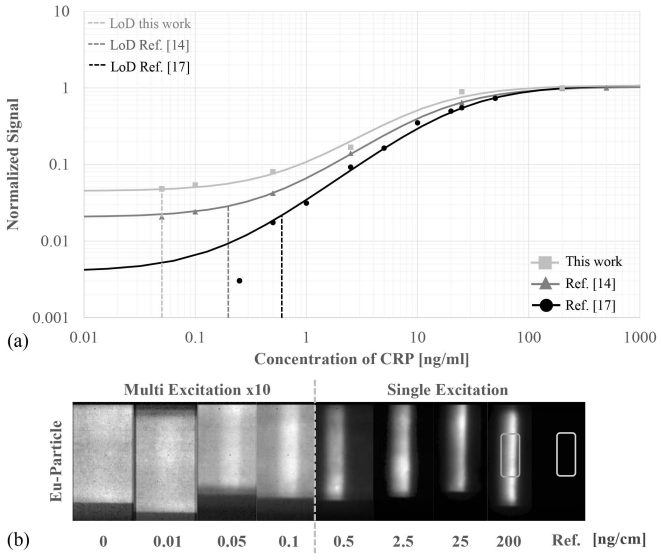

Fig. 13. (a) Normalized calibration curves of the LIP CIS based TRF reader (light grey, square) with a LoD of 0.05 ng/mL, of the CMOS sensor ASIC TRF reader from [14] (grey, triangle) with a LoD of 0.2 ng/mL and the commercial colorimetric LFA reader (black, dot) for different concentrations of CRP with a LoD of 0.7 ng/mL. The light grey and grey curves show Eu-based measurements with CRP concentrations of 200 ng/mL, 25 ng/mL, 2.5 ng/mL, 0.5 ng/mL, 0.1 ng/mL, 0.05 ng/mL, and the control (0 ng/mL). The black curve shows gold NP measurements with CRP concentrations of 200 ng/mL, 50 ng/mL, 25 ng/mL, 20 ng/mL, 10 ng/mL, 5 ng/mL, 2.5 ng/mL, 1 ng/mL, 0.5 ng/mL, 0.25 ng/mL, 0.1 ng/mL, and the control (0 ng/mL). (b) Images of the LIP CIS TRF reader for the measured concentrations and the reference for different excitation modes of single and x10 UV light excitation.

TABLE II
COMPARISON OF EXISTING OPTOELECTRONIC SENSOR SOLUTIONS FOR IMMUNOASSAY BASED POC APPLICATIONS

Reference	Application	Principle	Label / Signal generation	Technology	Pixel Array	Fill factor in %	DDR $\log_{10}(\cdot)$	LoD [ng/ml]	Overal CV in %
[18]	CRP detection	Chemo-luminescence Contact Sensing	HRP[(2)] + luminol conversion	0.5 µm CMOS	4 × 8	11.4	2.6[(4)]	400[(4)]	9[(5)]
[19]	HIV antibody detection	Absorption Contact Imaging	Gold NP + silver precipitate	0.35 µm CMOS	16 × 16	2	2	10000	15[(6)]
[20]	PSA[(1)] detection	Absorption Contact Sensing	HRP + TMB[(3)] conversion	0.35 µm CMOS	6 × 7	6.4	3	0.5	7
[21]	Influenza A nucleoprotein detection	Reflectometric LFA	Gold nanoparticle	0.35 µm CMOS	4 × 64	18	2.6	0.5	-
[17]	CRP detection	Reflectometric LFA	Gold nanoparticle	-	-	-	2.5	0.7	11
[13]	cTroponin I detection	TRF LFA	Eu particle	-	-	-	1	100	-
[22]	PCT[(7)] detection	TRF LFA Imaging	Eu particle	CCD[(8)]	640 x 480	-	2.7	0.08	8.6[(9)]
[24]	CRP detection	Fluorescence LFA	$mSiO_2$ UCNP[(10)]	-	-	-	3	0.05	< 5
[14]	CRP detection	TRF LFA	Eu particle	0.35 µm CMOS	5 × 5	11.7	3.3	0.2	26
This work	CRP detection	TRF LFA Imaging	Eu particle	0.18 µm CMOS	256 × 128	59	3.6	0.05	20

[(1)] Prostate specific antigen, [(2)] Horseradish peroxidase, [(3)] Tetramethylbenzidine, [(4)] Values for customized DDR for CRP Ab02 assay according to Fig. 4 (f) and Section 3.5 in [18], [(5)] Estimated value for customized DDR for CRP Ab02 assay according to Fig. 4 (f) in [18], [(6)] Estimated value for HIV antibody detection from Fig. 3 (c) in [19], [(7)] Procalcitonin, [(8)] Medisensor aQcare^{TM} TRF system, [(9)] Calculated average intra-assay precision. [(10)] Mesoporous silica ($mSiO_2$) coated up-converting nanoparticle (UCNP)

deviation (SD) of all control measurements for each LFA reader system.

The developed LIP CIS reader reaches the highest DDR and the best LoD not only in comparison to the commercially available colorimetric [17] as well as Eu-TRF LFA reader system [22] and to the CMOS sensor ASIC based TRF reader from [14], but also in relation to other prior-art optoelectronic sensor systems for immunoassay based PoC applications, see Table II.

V. DISCUSSION

The presented LIP CIS-based TRF reader system promises to improve the biochemical analysis process in PoC applications especially for the readout of LFA test strips.

Table II gives an overview of comparable prior work. The application cases must be compared very carefully because of their various measurement principles, the diverse analytes to be detected, and the different measurement setups with a variety of optical detectors. Regarding the analytes to be detected, a direct comparison of those systems in which CRP was detected is most meaningful, since the same analyte is involved. From the perspective of the principles used, a comparison of the fluorescence/luminescence-based systems would be more feasible. The table is primarily intended to illustrate the many and diverse technical system approaches and implementations, but also the improvements that, in combination with various immunological assays, enable the increasingly sensitive detection of analytes over an extended detection range.

Taken individually, the applications pursue the following goals: The DDR should ideally be as high as possible to span a wide range of analyte concentrations. In addition, immunoassay-based test systems aim to achieve the lowest possible LoD and CV with respect to their application. With regard to the aforementioned explanations, the LIP CIS-based TRF reader presented in this work shows the best performance in terms of the lowest LoD and highest DDR compared to state-of-the-art CMOS biochip contact imaging and contact sensing immunoassay approaches [18]–[20] as well as to commercially available Eu particle based TRF-LFA approaches [13], to our previous work [14] and to colorimetric LFA readers using gold NP [21].

The work in [24] shows comparable performance in terms of LoD and a better CV but cannot achieve such a high detection dynamic range compared to our work. We think, that the different excitation modes provide advantages especially when measuring higher concentrations up to 200 ng/mL compared to 50 ng/mL in [24]. Also, the preparation efforts for the mesoporous silica (mSiO2) coated up-converting nanoparticles (UCNPs) and the assay time of 8 min in [24] is comparable to the preparation of Eu chelate particles and the total assay time of 10 min in our work. Some disadvantages regarding the overall system design we see in the approach in [24] are: First, a near-infrared (NIR) laser is used, which is more expensive than the low cost LED light source used in our work. In addition, the light energy introduced must be higher to excite the fluorescent particles because the particles and analytes are in water, which absorbs NIR light and thus reduces the energy input. The used Eu particles with a diameter of 200 nm in our work are twice as large as the UCNPs. The advantage of the Eu chelate particles is, that much more dye complexes can be added to the particles. This results in a higher fluorescent signal and therefore improves the SNR. Finally, in [24] a 980 nm wavelentgh optical filter is needed to suppress the excitation light of the NIR laser. Our system concept and time-resolved readout approach with LED synchronization and active LED discharge makes it possible to dispense with optical filters and thus reduce system complexity and costs.

Furthermore, the image sensor based TRF measurement system shows that on the one hand the system complexity can be reduced, since in comparison to contact imaging and contact sensing applications no application specific CMOS biochip development with specialized assembly and immobilization of capture molecules directly on the sensor surface is required. In the setup of this work, standardized producible test strips can be used for the quantification of analytes and the image sensor is reusable. On the other hand, the large sensor array of 256 $\times$ 128 LIPs allows a high spatial resolution, which eases the alignment challenges regarding the LFA test strip with respect to the sensor system in contrast to detectors and sensor concepts with low spatial resolution.

CV and reproducibility can be further increased with fine adjustments and automation in the manufacturing process of the test strips. Optimization of the test strips also help to reduce the background signal, improve the SNR and thus the LoD. Further developments in the positioning accuracy of the test strips will enhance the validity and robustness of the measurement results.

VI. Conclusion

In this paper, we demonstrate the concept, design, and evaluation results of a LIP CIS-based reader system for quantitative immunoassay-based diagnostics using a TRF measurement principle. Measurements with Eu particles and CRP immunoassays were successfully performed with LFA test strips. The resulting fluorescence of Eu particles after excitation was imaged using the 256 $\times$ 128 large LIP CIS. The presented image sensor system is more robust to alignment errors for readout of LFA test strips than detectors with low spatial resolution.

For the validation with Eu fluorescence standards, the demonstrator system showed a very high DDR of 5.1 orders of magnitude and a LoD of 0.1 ng/cm. For the quantification of CRP, the LIP CIS-based TRF LFA reader demonstrated a high DDR of 3.6 orders of magnitude and an excellent LoD of 0.05 ng/mL. This is 4 times better then the LoD of the CMOS sensor ASIC based TRF reader from [14] with a LoD of 3.3 orders of magnitude and 14 times better than the LoD of the commercial LFA reader [17] with a DDR of 2.5 orders of magnitude. The overall CV of the LIP CIS TRF reader for the quantification of CRP is $20\,\%$.

Future work will optimize the LFA test strips and reduce the backround signal to further enhance SNR and the LoD. Moreover, reproducibility and CV can be improved with optimized positioning accuracy as well as fine adjustments and automation in the manufacturing process of the LFA test strips.

Acknowledgment

The authors thank Sven Engelhardt and Sebastian Uziel from IMMS Institut für Mikroelektronik- und Mechatronik-Systeme gemeinnützige GmbH (IMMS GmbH), Ilmenau, Germany, for their contributions to the development of the hardware of the demonstrator system.

References

[1] D. S. Ong, S. de Man, F. A. Lindeboom, and J. G. Koeleman, "Comparison of diagnostic accuracies of rapid serological tests and ELISA to molecular diagnostics in patients with suspected coronavirus disease 2019 presenting to the hospital," *Clin. Microbiol. Infection*, vol. 26, no. 8, pp. 1094–e7–1094.e10, 2020.

[2] A. E. Urusov, A. V. Zherdev, and B. B. Dzantiev, "Towards lateral flow quantitative assays: Detection approaches," *Biosensors*, vol. 9, no. 3, 2019, Art. no. 89.

[3] X. Gong et al., "A review of fluorescent signal-based lateral flow immunochromatographic strips," *J. Mater. Chem. B*, vol. 5, pp. 5079–5091, 2017.

[4] J. Yuan and G. Wang, "Lanthanide complex-based fluorescence label for time-resolved fluorescence bioassay," *J. Fluorescence*, vol. 15, no. 4, pp. 559–568, 2005.

[5] S. Webb et al., "A wide-field time-domain fluorescence lifetime imaging microscope with optical sectioning," *Rev. Sci. Instruments*, vol. 73, no. 4, pp. 1898–1907, 2002.

[6] M.-W. Seo, Y. Shirakawa, Y. Kawata, K. Kagawa, K. Yasutomi, and S. Kawahito, "A time-resolved four-tap lock-in pixel CMOS image sensor for real-time fluorescence lifetime imaging microscopy," *IEEE J. Solid-State Circuits*, vol. 53, no. 8, pp. 2319–2330, Aug. 2018.

[7] A. Diéguez, J. Canals, N. Franch, J. Diéguez, O. Alonso, and A. Vilá, "A compact analog histogramming SPAD-based CMOS chip for time-resolved fluorescence," *IEEE Trans. Biomed. Circuits Syst.*, vol. 13, no. 2, pp. 343–351, Apr. 2019.

[8] Y. Maruyama and E. Charbon, "An all-digital, time-gated 128x128 spad array for on-chip, filter-less fluorescence detection," in *Proc. Proc. 16th Int. Solid-State Sensors, Actuators Microsystems Conf.*, 2011, pp. 1180–1183.

[9] C. Lee, B. Johnson, T. Jung, and A. Molnar, "A 72 $\times$ 60 angle-sensitive SPAD imaging array for lens-less flim," *Sensors*, vol. 16, no. 9, 2016, Art. no. 1422.

[10] M. A. Al-Rawhani et al., "Multimodal integrated sensor platform for rapid biomarker detection," *IEEE Trans. Biomed. Eng.*, vol. 67, no. 2, pp. 614–623, Feb. 2020.

[11] R. Wilson, "Sensitivity and specificity: Twin goals of proteomics assays. can they be combined?," *Expert Rev. Proteomic.*, vol. 10, no. 2, pp. 135–149, 2013.

[12] R. M. Field, S. Realov, and K. L. Shepard, "A 100 fps, time-correlated single-photon-counting-based fluorescence-lifetime imager in 130 nm CMOS," *IEEE J. Solid-State Circuits*, vol. 49, no. 4, pp. 867–880, Apr. 2014.

[13] S. Karthik, M. I. Shah, S. Natarajan, M. J. Shetty, and J. Joseph, "A motion free image based TRF reader for quantitative immunoassay," in *Proc. IEEE Healthcare Innovations Point Care Technol.*,(HI-POCT), 2019, pp. 163–166.

[14] A. Hofmann et al., "Filterless TRF reader with CMOS sensor ASIC for lateral flow immunoassays," in *Proc. IEEE Biomed. Circuits Syst. Conf. (BioCAS)*, 2021, pp. 1–6.

[15] M.-W. Seo and S. Kawahito, "A 7 ke-SD-FWC 1.2 e-RMS temporal random noise 128 $\times$ 256 time-resolved CMOS image sensor with two in-pixel SDs for biomedical applications," *IEEE Trans. Biomed. Circuits Syst.*, vol. 11, no. 6, pp. 1335–1343, Dec. 2017.

[16] B. D. Plikaytis, S. Turner, L. Gheesling, and G. Carlone, "Comparisons of standard curve-fitting methods to quantitate neisseria meningitidis group a polysaccharide antibody levels by enzyme-linked immunosorbent assay," *J. Clin. Microbiol.*, vol. 29, no. 7, pp. 1439–1446, 1991.

[17] Qiagen, "aLF Reader User Manual," 2017. [Online]. Available: https://www.alf-reader.com/wp-content/uploads/sites/9/2017/07/ESLR12-DH-1001-User-Manual-aLF-Reader-EN-01-.pdf

[18] H. Klapproth et al., "Development of a multi-analyte CMOS sensor for point-of-care testing," *Sens. Bio-Sens. Res.*, vol. 5, pp. 117–122, 2015.

[19] B. Nagy, M. A. Al-Rawhani, B. C. Cheah, M. P. Barrett, and D. R. Cumming, "Immunoassay multiplexing on a complementary metal oxide semiconductor photodiode array," *ACS Sensors*, vol. 3, no. 5, pp. 953–959, 2018.

[20] A. Hofmann, M. Meister, A. Rolapp, P. Reich, F. Scholz, and E. Schäfer, "Light-controlled photometer with optoelectronic CMOS biochip for quantitative PSA detection," in *Proc. IEEE Int. Symp. Circuits Syst. (ISCAS)*, 2020, pp. 1–5.

[21] E. Pilavaki, V. Valente, and A. Demosthenous, "CMOS image sensor for lateral flow immunoassay readers," *IEEE Trans. Circuits Syst. II: Exp. Briefs*, vol. 65, no. 10, pp. 1405–1409, 2018.

[22] X.-Y. Shao, C.-R. Wang, C.-M. Xie, X.-G. Wang, R.-L. Liang, and W.-W. Xu, "Rapid and sensitive lateral flow immunoassay method for procalcitonin (PCT) based on time-resolved immunochromatography," *Sensors*, vol. 17, no. 3, 2017, Art. no. 480.
[23] G. T. Hermanson, *Bioconjugate Techniques*, 2nd ed. Amsterdam, The Netherlands: Elsevier, 2008.
[24] J. Guo, S. Chen, S. Tian, K. Liu, X. Ma, and J. Guo, "A sensitive and quantitative prognosis of c-reactive protein at picogram level using mesoporous silica encapsulated core-shell up-conversion nanoparticle based lateral flow strip assay," *Talanta*, vol. 230, 2021, Art. no. 122335.

Alexander Hofmann received the B.Sc. and M.Sc. degrees in biomedical engineering from the Ilmenau University of Technology, Ilmenau, Germany, in 2010 and 2012, respectively. He is currently working toward the Ph.D. degree. In 2012, he joined IMMS Institut für Mikroelektronik- und Mechatronik-Systeme gemeinnützige GmbH, Ilmenau, where he develops analog integrated circuits for bio-analytical and biomedical sensors and systems. His main research interests include mixed-signal integrated circuits, Lab-on-Chip, and CMOS biochip systems for bio-analytical and Point-of-Care applications.

Benjamin Saft received the B.Sc. and M.Sc. degrees in electrical engineering and information technology from the Ilmenau University of Technology, Ilmenau, Germany, in 2010 and 2012, respectively. In 2012, he joined IMMS Institut für Mikroelektronik- und Mechatronik-Systeme gemeinnützige GmbH, Ilmenau, Germany, where he is currently working as an Analog Design Engineer and a Project Manager. His research focuses on the development optoelectronic ASICs for novel Point-of-Care applications.

Peggy Reich received the master's degree in biosystems technology from the Technical University of Applied Sciences Wildau, Wildau, Germany, in 2008, and the Ph.D. degree in natural sciences from the Leibniz University of Hannover, Hanover, Germany, in 2020 for the development of an impedimetric aptasensor for the detection of Staphylococcus aureus. After working in Finland with the VTT with prostate tumour cell lines and Post Graduate studies in South America, she was a Scientist with the Institute for Bioprocessing and Analytical measurement techniques in Germany. From 2018 to 2021, she was working at IMMS Institut für Mikroelektronik- und Mechatronik-Systeme gemeinnützige GmbH, Ilmenau, Germany, as a Project Manager and by generating new business projects.

Martin Grabmann received the B.Sc. and M.Sc. degrees in computer engineering from Ilmenau University of Technology, Ilmenau, Germany, in 2015 and 2017, respectively. He is currently working toward the Ph.D. degree. In 2017, he joined IMMS Institut für Mikroelektronik- und Mechatronik-Systeme gemeinnützige GmbH, Ilmenau, where he is responsible for mixed-signal integrated circuit verification. His main research focuses on modeling methodology for design verification.

Georg Gläser received the M.Sc. degree in electrical engineering from the Ilmenau University of Technology, Ilmenau, Germany, in 2013. In 2013, he joined IMMS Institut für Mikroelektronik- und Mechatronik-Systeme gemeinnützige GmbH (IMMS GmbH), Ilmenau, and is responsible for design methodology research and the development of digital circuits and systems.

Max Trübenbach received the B.Eng. and M.Sc. degrees in biotechnology and pharmaceutical biotechnology from the Ernst-Abbe-University of Applied Sciences, Jena, Germany, in 2018 and 2021. In 2020, he joined Senova Gesellschaft für Biowissenschaft und Technik mbH, Weimar, Germany, with the Research and Development Department and is currently a Scientist with several interdisciplinary projects. His research interests include the development of novel Point-of-Care applications and a digital Lateral Flow platform.

Alexander Rolapp received the diploma engineering degree in computer science engineering from Ilmenau University of Technology, Ilmenau, Germany, in 2007. He is currently a Scientific Assistant with IMMS Institut für Mikroelektronik- und Mechatronik-Systeme gemeinnützige GmbH, Ilmenau. His research interests include low power multisensor wireless applications and biomedical diagnostic sensor integration.

Marco Reinhard received the Diploma engineering degree in electrical engineering and information technology from the Ilmenau University of Technology, Ilmenau, Germany, in 2003. He is currently a Scientific Assistant with IMMS Institut für Mikroelektronik- und Mechatronik-Systeme gemeinnützige GmbH, Ilmenau. His research interests include electrostatic-discharge events with transmission-line pulse (TLP), and human-body model (HBM) tests.

Friedrich Scholz received the Diploma in chemistry and the Ph.D. degree from Friedrich-Schiller-University Jena, Jena, Germany, in 2009 and 2014, respectively. Since 2013, he has been a Research Assistant with Senova Gesellschaft für Biowissenschaft und Technik mbH in the development of novel and rapid diagnostic test systems. He is currently responsible for the Research and Development Department and working in several international and national interdisciplinary projects. His research focuses on new types of technology components in order to fundamentally improve the test systems.

Eric Schäfer received the B.Sc. and M.Sc. degrees in electrical engineering and information technology from the Ilmenau University of Technology, Ilmenau, Germany, in 2009 and 2010, respectively. In 2011, he joined IMMS Institut für Mikroelektronik- und Mechatronik-Systeme gemeinnützige GmbH, Ilmenau, where he currently heads the Microelectronics Team.